[6] Y. Xing, F. Ichida, T. Matsuoka, T. Isobe, Y. Ikemoto, T. Higaki, T. Tsuji, N. Haneda, A. Kuwabara, R. Chen, T. Futatani, S. Tsubata, S. Watanabe, K. Watanabe, K. Hirono, K. Uese, T. Miyawaki, K.R. Bowles, N.E. Bowles, J.A. Towbin, Genetic analysis in patients with left ventricular noncompaction and evidence for genetic heterogeneity, Mol. Genet. Metab. 88 (2006) 71–77.

[7] Q. Wang, J. Shen, I. Splawski, D. Atkinson, Z. Li, J.L. Robinson, A.J. Moss, J.A. Towbin, M.T. Keating, SCN5A mutations associated with an inherited cardiac arrhythmia, long QT syndrome, Cell 80 (1995) 805–811.

[8] C. Bezzina, M.W. Veldkamp, M.P. van Den Berg, A.V. Postma, M.B. Rook, J.W. Viersma, I.M. van Langen, G. Tan-Sindhunata, M.T. Bink-Boelkens, A.H. van Der Hout, M.M. Mannens, A.A. Wilde, A single Na(+) channel mutation causing both long-QT and Brugada syndromes, Circ. Res. 85 (1999) 1206–1213.

[9] M. Vatta, R. Dumaine, G. Varghese, T.A. Richard, W. Shimizu, N. Aihara, K. Nademanee, R. Brugada, J. Brugada, G. Veerakul, H. Li, N.E. Bowles, P. Brugada, C. Antzelevitch, J.A. Towbin, Genetic and biophysical basis of sudden unexplained nocturnal death syndrome (SUNDS), a disease allelic to Brugada Syndrome, Hum. Mol. Genet. 11 (2002) 337–345.

[10] Q. Chen, G.E. Kirsch, D. Zhang, R. Brugada, J. Brugada, P. Brugada, D. Potenza, A. Moya, M. Borggrefe, G. Breithardt, R. Ortiz-Lopez, Z. Wang, C. Antzelevitch, R.E. O'Brien, E. Schulze-Bahr, M.T. Keating, J.A. Towbin, Q. Wang, Genetic basis and molecular mechanism for idiopathic-ventricular fibrillation, Nature 392 (1998) 293–296.

[11] D.W. Benson, D.W. Wang, M. Dyment, T.K. Knilans, F.A. Fish, M.J. Strieper, T.H. Rhodes, A.L. George, Congenital sick sinus syndrome caused by recessive mutations in the cardiac sodium channel gene (SCN5A), J. Clin. Invest. 112 (2003) 1019–1028.

[12] J.J. Schott, C. Alshinawi, F. Kyndt, V. Probst, T.M. Hoorntje, M. Hulsbeek, A.A. Wilde, D. Escande, M.M. Mannens, H. Le Marec, Cardiac conduction defects associate with mutations in SCN5A, Nat. Genet. 23 (1999) 20–21.

[13] D.W. Wang, Desai, R. Reshma, L. Crotti, M. Arnestad, R. Insolia, M. Pedrazzini, C. Ferrandi, A. Vege, T. Rognum, P.J. Schwartz, A.L. George, Cardiac sodium channel dysfunction in sudden infant death syndrome, Circulation 115 (2007) 368–376.

[14] W.P. McNair, L. Ku, M.R. Taylor, P.R. Fain, D. Dao, E. Wolfel, L. Mestroni, Familial Cardiomyopathy Registry Research Group, SCN5A mutation associated with dilated cardiomyopathy, conduction disorder, and arrhythmia, Circulation 110 (2004) 2163–2167.

[15] T.M. Olson, V.V. Michels, J.D. Ballew, S.P. Reyna, M.L. Karst, K.I. Herron, S.C. Horton, R.J. Rodeheffer, J.L. Anderson, Sodium channel mutations and susceptibility to heart failure and atrial fibrillation, JAMA 293 (2005) 447–454.

[16] M. Bienengraeber, T.M. Olson, V.A. Selivanov, E.C. Kathmann, F. O'Cochlain, F. Gao, A.B. Karger, J.D. Ballew, D.M. Hodgson, L.V. Zingman, Y. Pang, A.E. Alekseev, A. Terzic, ABCC9 mutations identified in human dilated cardiomyopathy disrupt catalytic $K_{ATP}$ channel gating, Nat. Genet. 36 (2004) 382–387.

[17] I. Splawski, K.W. Timothy, M. Tateyama, C.E. Clancy, A. Malhotra, A.H. Beggs, F.P. Cappuccio, G.A. Sagnella, R.S. Kass, M.T. Keating, Variant of SCN5A sodium channel implicated in risk of cardiac arrhythmia, Science 297 (2002) 1333–1336.

[18] L. Gouas, V. Nicaud, M. Berthet, A. Forhan, L. Tiret, B. Balkau, P. Guicheney, D.E.S.I.R. Study Group, Association of KCNQ1, KCNE1, KCNH2 and SCN5A polymorphisms with QTc interval length in a healthy population, Eur. J. Hum. Genet. 13 (2005) 1213–1222.

[19] C.R. Bezzina, W. Shimizu, P. Yang, T.T. Koopmann, M.W. Tanck, Y. Miyamoto, S. Kamakura, D.M. Roden, A.A. Wilde, Common sodium channel promoter haplotype in asian subjects underlies variability in cardiac conduction, Circulation 113 (2006) 338–344.

[20] N. Makita, H. Tsutsui, Genetic polymorphisms and arrhythmia susceptibility, Circ. J. Suppl. A (2007) A54–A60.

[21] K. Maekawa, Y. Saito, S. Ozawa, S. Adachi-Akahane, M. Kawamoto, K. Komamura, W. Shimizu, K. Ueno, S. Kamakura, N. Kamatani, M. Kitakaze, J. Sawada, Genetic polymorphisms and haplotypes of the human cardiac sodium channel α subunit gene (SCN5A) in Japanese and their association with arrhythmia, Ann. Hum. Genet. 69 (2005) 413–428.

[22] E. Schulze-Bahr, L. Eckardt, G. Breithardt, K. Seidl, T. Wichter, C. Wolpert, M. Borggrefe, W. Haverkamp, Sodium channel gene (SCN5A) mutations in 44 index patients with Brugada syndrome: different incidences in familial and sporadic disease, Hum. Mutat. 6 (2003) 651–652. Erratum in: Hum. Mutat. 1 (2005) 61.

[23] F. Ichida, Y. Hamamichi, T. Miyawaki, Y. Ono, T. Kamiya, T. Akagi, H. Hamada, O. Hirose, T. Isobe, K. Yamada, S. Kurotobi, H. Mito, T. Miyake, Y. Murakami, T. Nishi, M. Shinohara, M. Seguchi, S. Tashiro, H. Tomimatsu, Clinical features of isolated noncompaction of the ventricular myocardium: long-term clinical course, hemodynamic properties, and genetic background, J. Am. Coll. Cardiol. 34 (1999) 233–240.

[24] T.J. Bunch, M.J. Ackerman, Promoting arrhythmia susceptibility, Circulation 113 (2006) 330–332.

[25] P.C. Viswanathan, D.W. Benson, J.R. Balser, A common SCN5A polymorphism modulates the biophysical effects of an SCN5A mutation, J. Clin. Invest. 111 (2003) 341–346.

[26] B. Ye, C.R. Valdivia1, M.J. Ackerman, J.C. Makielski, A common human SCN5A polymorphism modifies expression of an arrhythmia causing mutation, Physiol. Genomics 12 (2003) 187–193.

[27] B.H. Tan, C.R. Valdivia1, B.A. Rok, B. Ye, K.M. Ruwaldt, D.J. Tester, M.J. Ackerman, J.C. Makielski, Common human SCN5A polymorphisms have altered electrophysiology when expressed in Q1077 splice variants, Heart Rhythm 7 (2005) 741–747.

[28] O. Staub, D. Rotin, Regulation of ion transport by protein–protein interaction domains, Curr. Opin. Nephrol. Hypertens. 5 (1997) 447–454.

Biochemical and Biophysical Research Communications 378 (2009) 589–594

Contents lists available at ScienceDirect

Biochemical and Biophysical Research Communications

journal homepage: www.elsevier.com/locate/ybbrc

# Evaluation of channel function after alteration of amino acid residues at the pore center of KCNQ1 channel

Taruna Ikrar [a,b], Haruo Hanawa [a], Hiroshi Watanabe [a], Yoshiyasu Aizawa [a,*], Mahmoud M. Ramadan [a], Masaomi Chinushi [a], Minoru Horie [c], Yoshifusa Aizawa [a]

[a] Division of Cardiology, First Department of Internal Medicine, Niigata University Graduate School of Medical and Dental Sciences, 1-754 Asahimachi Dori, Chuo-ku, Niigata 951-8510, Japan
[b] The National Agency for Drug and Food Control, Republic of Indonesia, Jakarta, Indonesia
[c] Department of Cardiovascular and Respiratory Medicine, Shiga University of Medical Science, Shiga, Japan

ARTICLE INFO

*Article history:*
Received 17 November 2008
Available online 3 December 2008

*Keywords:*
Long QT syndrome
Missense mutation
KCNQ1
$I_{Ks}$
Pore center
Amino acid residue

ABSTRACT

The effect of the electrical charge or the size of the amino acid residue at the pore center of a slowly activation component of the delayed rectifier potassium channel: KCNQ1 was studied. $K^+$ currents were measured after transfection of one of four KCNQ1 mutants: substituting Isoleucine with Lysine, Glutamate, Valine or Glycine and then transfected in COS-7 cells. Both the negatively- and positive charged residue I313 K and I313E showed a loss of function when expressed alone and a dominant negative suppression when co-expressed with wild type KCNQ1. When the site was substituted with the smallest neutral amino acid residue: I313G, there was a small reduction of current when transfected alone and a gain of function when co-transfected with the wild type. I313V showed no difference from the wild type. Changes of amino acid residue at the pore center of KCNQ1 may alter the channel function but this depends on the electrical charge or the size of amino acid residue.



The delayed rectifier $K^+$ current ($I_{Ks}$) channel is formed by the co-assembly of KCNQ1 (KvLQT1) with KCNE1 (minK) and contributes to repolarizing cardiac myocytes [1]. A mutation in either subunit is well known to cause long QT syndrome (LQTS) which predisposes affected individuals to cardiac arrhythmias and sudden death [2,3].

In LQTS, the phenotype was suggested to be affected by the site of the mutation and patients with trans-membrane mutations had more frequent diagnostic criteria, LQTS-related cardiac events and a prolonged QT-interval after exercise than patients with a C-terminal mutation [4]. However, this finding from Japan is in contrast to that of the International Long QT Syndrome Registry in which the phenotypes were not related to the site of the mutation [5].

We have previously characterized the physiological consequences of the LQTS-associated mutation at the pore center: I313K, in a patient with a severe LQT1 phenotype [6]. The mutant channels showed almost no current when transfected alone but when co-expressed with WT-KCNQ1, they showed a dominant negative suppression [6].

In this report, our aim was to explore the effects of the charge and the size of the amino acid residue at the pore center of KCNQ1. In order to do this, we substituted its Isoleucine residue with electrically charged ones: Lysine and Glutamate and two neutral amino acids: Valine and Glycine, and performed an electrophysiological study after transfection of each mutant.

## Materials and methods

*Construction of plasmid DNA for gene transfer.* A full-length human WT-KCNQ1, KCNE1, and mutant KCNQ1 were inserted into a plasmid vector pIRES2-EGFP using BamHI restriction sites making the pIRES2-EGFP-KCNQ1, pIRES-EGFP-KCNE1, and mutant pIRES2-EGFP-I313K plasmids as described previously [6]. In the pIRES2-EGFP-I313K plasmid, we introduced three new missense mutations which can occur in humans. One is a mutant with Glutamate which is a positively charged large amino acid residue (I313E). Then we prepared two mutants, Valine (I313V), a neutral amino acid of similar size and homology to the Isoleucine residue in WT-KCNQ1 [7–10] and Glycine as the smallest sized neutral amino acid (I313G).

The mutation of I313E was introduced with a PCR reaction using the mutant primer sets: 5′-GTGGTCACAGTCACCAC*gaa*GGCTATGG GGACAAGGTG-3′ and 5′-CACCTTGTCCCCATAGCC*ttc*GGTGGTGACTG TGACCAC-3′ (*lower case letters indicate mutation sites*). The mutation of I313V was introduced with a PCR using the mutant primer sets 5′-GTGGTCACAGTCACCAC*gtc*GGCTATGGGGACAAGGTG-3′ and 5′-CA CCTTGTCCCCATAGCC*gac*GGTGGTGACTGTGACCAC-3. For the mutation of I313G, we used the primer sets 5′-GTGGTCACAGTCACCA

* Corresponding author. Fax: +81 25 228 5611.
*E-mail address:* aizaways@med.niigata-u.ac.jp (Y. Aizawa).

0006-291X/$ - see front matter © 2008 Elsevier Inc. All rights reserved.
doi:10.1016/j.bbrc.2008.11.076

CCggcGGCTATGGGGACAAGGTG-3′ and 5′-CACCTTGTCCCCATAGC CgccGGTGGTGACTGTGACCAC-3′.

For these experiments, we used the QuickChange site-directed mutagenesis kit (Stratagene, La Jolla, CA, USA). The resulting products were again amplified by PCR using the primers 5′-CCATTTCCATC ATCGACCTCA-3′ and 5′-AAGGAGAGCGCTGGTGAAG-3′. This final PCR product was ligated to the pIRES2-EGFP WT-KCNQ1 vector using the PstI sites at nucleotide positions 697 and 1675 of KCNQ1. The PCR insert was also cleaved with PstI prior to ligation. The resulting four cloned plasmids were then transformed into *Escherichia coli* JM109 competent cells and purified using a Quantum Prep Plasmid Maxi prep kit (Bio-Rad Laboratories, Hercules, CA).

*Culture and transfection of COS-7 cells.* A COS-7 monkey kidney cell line was obtained from the American Type Cell Collection and cultured in Dulbecco's modified Eagles medium (Invitrogen Corporation, Gibco-BRL, Rockville, MD) supplemented with 1% penicillin–streptomycin (prepared with 10,000 U/ml penicillin G sodium and 10,000 μg/ml streptomycin sulfate in 0.85% saline) and 10% fetal bovine serum in a humidified 5% $CO_2$ incubator at 37 °C. The number of cells seeded per ml of medium was $2 \times 10^5$ on average. Cultured cells were seeded in 60 mm plates 24 h before transfection, then transiently transfected with various plasmids by the Fugene-6 method (Roche Applied Science, Indianapolis, IN).

*Electrophysiological experiments.* The whole-cell patch-clamp method was applied to COS-7 cells transfected with the wild type and/or mutant plasmids as described previously [6,11,12]. Briefly, cells were allowed to settle at the bottom of a bath (0.5 ml) mounted on an inverted microscope (Olympus Corp., Tokyo, Japan). Cells were superfused with the bath solution (140 mmol NaCl, 5.4 mmol KCl, 0.5 mmol $MgCl_2$, 1.8 mmol $CaCl_2$, 0.33 mmol $NaH_2PO_4$, 5.5 mmol glucose and 5 mmol HEPES) and the pH was adjusted to 7.4 by using NaOH. When inserted into the cell/bath solution, a glass pipette with an internal diameter of 1.0–1.5 μm had a resistance of 4–6 MΩ when filled with the following internal solution: 100 mmol/l K-aspartate, 20 mmol/l KCl, 5 mmol/l ATP-Mg, 5 mmol/l phosphocreatine-dipotassium, 5 mmol/l EGTA, 5 mmol/l HEPES and 1 mmol/l $CaCl_2$ (the pH was adjusted to 7.2 with KOH). A patch-clamp amplifier Axopatch 200B (Axon Instruments, Foster City, CA) was used to record membrane currents.

After obtaining a whole-cell configuration, cell membrane capacitance was estimated by analyzing the transient capacitance elicited by 5 mV hyperpolarizing pulses. Cells were held at a starting potential of −80 mV and depolarizing pulses of various potentials ranging from −80 to +80 mV in 20 mV increments for 2 s were applied, followed by repolarization to −40 mV for 2 s to record tail currents. The pCLAMP 8.0 software (Axon Instruments, Foster City, CA) was used to generate the pulse protocol, data acquisition, and analyses.

To be confident of the currents obtained, our analyses only included recordings obtained by Giga-seal after applying the following quality control criteria for the patch-clamp technique [13]: (1) the starting seal resistance was required to be more than 1 GΩ, (2) the series resistance was required to be lower than 20 MΩ throughout the recording, (3) the membrane potential was required to be at a higher negative level than −50 mV if normal high-potassium intracellular solution was used; and (4) cell capacitance and resistance were required to be stable. Furthermore, to check the quality of our findings, COS-7 cells transfected with wild type KCNQ1 were compared with the results of Barhanin et al. [1] and Sanguinetti et al. [15] regarding the properties and biophysical characteristics of the wild type KCNQ1 potassium current.

*Data analyses.* Analyses of the data were performed with Clampfit 9.1 (Axon Instruments, Foster City, CA) and SPSS for Windows ver.15 (SPSS Inc., Chicago, IL). The time constants for activation and deactivation were determined by fitting the current recordings with a single-exponential function [16]: $f(t) = A_0 + A\,exp(-t/\tau)$ and the voltage dependence of channel activation and deactivation were fitted with the Boltzmann equation: $I = I_{max}/(1 + exp[(V_{1/2} - V)/k])$, where $A$ was current amplitude, $\tau$ was the time constant, $t$ was time, $I$ was current amplitude, $I_{max}$ was the maximal tail current, $V$ was the test pulse potential, $V_{1/2}$ was the half-maximal activation potential, and $k$ was the slope of the activation curve. The relationship of current density with side-chain residue volume was measured after 2 s during depolarization.

Results for continuous normal data were expressed as mean ± standard error of estimation. The comparison of means of continuous normal variables across a grouping variable with two levels was done using the student's $t$-test and the comparison of means of continuous normal variables across a grouping variable with several levels was undertaken with one-way analysis of variance (ANOVA). A two-sided significance level of 0.05 was used for all analyses.

## Results

### *Wild type and mutant channel currents*

The cells transfected with KCNQ1 and KCNE1 exhibited a slowly activated outward current compatible with $I_{Ks}$ from native cardiac myocytes. Each mutant was then transfected with KCNE1 and the current–voltage relationships of the peak current during depolarization and the tail current were measured as Fig. 1.

I313 G ($n = 17$ cells) showed an approximately 20% reduction in peak current and the densities of the peak and tail currents were less than those of the wild type ($n = 10$ cells) but the differences were not significant ($P = 0.987$). The activation curve shifted towards the left (Fig. 1A, B, F and Table 1). I313V ($n = 15$ cells) exhibited no significant change in the current compared to those of the wild type ($P = 1.00$, Fig. 1A–C and F). The shape of the membrane potential vs. the current density curve was also similar among cells transfected with the wild type and I313V ($P = 1.00$, Fig. 1F and G).

I313K ($n = 14$ cells) produced almost no current and I313E ($n = 15$ cells) showed a marked reduction of current compared to the wild type ($P < 0.01$ for both, Fig. 1A, D, E and Table 1).

### *Co-expression of WT and mutant KCNQ1 channels*

Cells were then co-transfected with 0.5 μg of each mutant and 0.5 μg of the wild type together with KCNE1 (Fig. 2). Co-transfection of I313 G with the wild type ($n = 16$ cells) showed a 2-fold increase of the current compared to the cells transfected with the wild type: 110.7 ± 4.7 vs. 57.1 ± 6.2 pA/pF ($P < 0.001$) (Fig. 2A and B) and the tail current was also significantly augmented: 26.2 ± 1.7 vs. 16.0 ± 2.3 pA/pF ($P < 0.05$). The activation curve was shifted towards the left (Fig. 2E and F). I313 V co-transfected with the wild type ($n = 9$ cells) showed similar current i ıtensities without significant differences ($P = 1.00$) compared to the wild type ($n = 11$ cells) (Fig. 2A, C and Table 1). Co-transfection of I313E with the wild type ($n = 15$ cells) exhibited a similar current to that of cells co-transfected with I313 K and the wild type ($n = 14$ cells) both showing >70% reduction of current amplitude compared to the wild type ($P < 0.001$) (Fig. 2D–E, and Table 1). An increased current in I313G with the wild type suggested a gain of function and a markedly reduced current in I313E and I313K when co-expressed with the wild type would reflect a dominant negative suppression (Fig. 2F–G).

### *Kinetic analysis of mutant KCNQ1 channels*

The hetero-tetrameric of the wild type and mutant channel in the presence of KCNE1 showed peak and tail currents which were well fitted with the Boltzmann equation or a single-exponential

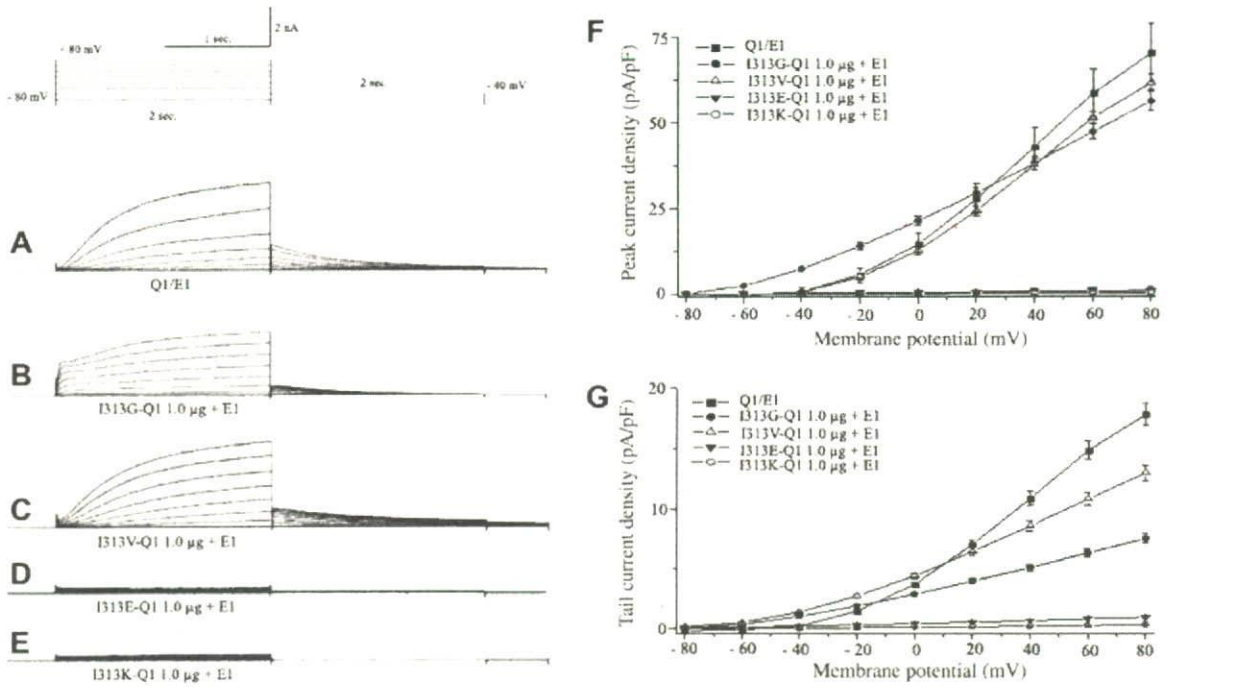


**Fig. 1.** Results of the whole-cell patch-clamp experiments in COS-7 cells. COS-7 cells were transfected with plasmids of wild type KCNQ1 (Q1) and four mutants together with (E1)KCNE1 (A–E). The activation is rapid but the peak current was about 20% smaller in I313G (B) compared with the wild type (A). I313K and I313E showed almost no current (D,E). The current–voltage relationships of cells transfected with five plasmids are shown on the right and a shift to the left can be seen in I313G (F). The differences in the peak and tail currents among the wild type and four mutants were not significant. Pulse protocol and graph scale are shown at the top.

**Table 1**
Comparison of kinetics and peak currents in COS-7 cells transfected with wild type and/or mutant KCNQ1 plasmids.

| Plasmid DNA | Peak current | Activation curve (mV) | | Time constants (τ, ms) | |
|---|---|---|---|---|---|
| | (pA/pF) | (V1/2) | Slope (*k*) | Activation | Deactivation |
| WT 1.0 ng (*n* = 10) | 70.4 ± 8.7 2 | 17.0 ± 1.4 | 17.0 ± 1.4 | 1252.0 ± 14.2 | 2.0 ± 14.2220 |
| I313G 1.0 ng (*n* = 17) | 56.4 ± 2.7[†] | 17.6 ± 1.3[‡] | 19.9 ± 1.2[†] | 607.4 ± 5.2[‡] | 397.2 ± 14.5[†] |
| I313V 1.0 ng (*n* = 15) | 61.8 ± 2.2[†] | 20.9 ± 1.6[†] | 17.3 ± 1.1[†] | 1389.6 ± 5.7[†] | 369.3 ± 110.6[†] |
| I313E 1.0 ng (*n* = 15) | 0.9 ± 1.1[‡] | – | – | – | – |
| I313K 1.0 ng (*n* = 14) | 0.4 ± 0.2[‡] | – | – | – | – |
| WT[#] (*n* = 11) | 57.1 ± 6.2 | 23.2 ± 1.3 | 16.7 ± 1.1 | 1154.3 ± 62.8 | 213.6 ± 11.85 |
| WT/I313G (*n* = 16) | 110.7 ± 4.7[*] | 15.6 ± 1.2[*] | 20.2 ± 1.3[*] | 350.8 ± 3.0[*] | 648.4 ± 126.0[*] |
| WT/I313V (*n* = 9) | 59.5 ± 1.5[§] | 22.5 ± 1.1[§] | 16.9 ± 1.0[§] | 1297.5 ± 5.7[§] | 327.53 ± 110.6[§] |
| WT/I313E (*n* = 15) | 9.3 ± 0.5[*] | 19.0 ± 1.1[§] | 18.1 ± 1.0[§] | 1242.2 ± 91.4[§] | 289.0 ± 74.4[§] |
| WT/I313K (*n* = 14) | 14.6 ± 1.7[*] | 23.9 ± 1.8[§] | 17.1 ± 1.6[§] | 1302.1 ± 88.2[§] | 388.4 ± 64.4[§] |

Data represents the mean ± SEM.
WT, wild type; KCNQ1 (α subunit of the potassium voltage-gated channel KQT-like subfamily member 1); KCNE1, β subunit of the potassium voltage-gated channel $I_{Ks}$-related family member 1; I313K;I313E;I313V and I313G: mutant KCNQ1.
[‡] $P < 0.01$ vs. WT 1.0 μg/KCNE1 1.0 μg.
[†] $P > 0.05$ vs. WT 1.0 μg/KCNE1 1.0 μg.
[#] 0.5 μg of WT was transfected and subsequent study was transfected 0.5 μg of mutant.
[*] $P < 0.001$ vs. WT 0.5 μg/KCNE1 1.0 μg.
[§] $P > 0.05$ vs. WT 0.5 μg/KCNE1 1.0 μg. Each plasmid was transfected with KCNE1 (see text).

function [16]. The activation curves for cells transfected with the wild type and that of co-transfection with I313K, I313E or I313V were not significantly different (Table 1).

Expression of I313G alone showed a more rapid initial activation compared to the wild type: 607.4 ± 5.2 vs. 1252.0 ± 14.2 ms ($P < 0.01$) and smaller $V_{1/2}$: 17.6 ± 1.3 vs. 23.5 ± 1.4 mV ($P < 0.01$) as shown in Fig. 1 and Table 1. I313 G co-transfected with the wild type showed a significant shift in the activation curve towards the left compared with the wild type and the time constant of activation was smaller: 350.8 ± 3.0 vs. 1154.3 ± 62.8 ms ($P < 0.001$) while that of deactivation of the tail current was larger: 648.4 ± 126.0 vs. 213.6 ± 11.85 ms ($P < 0.001$) as shown in Fig. 2A and B, Table 1).

The activation curves for cells transfected with I313E, I313K and I313V together with the wild type revealed statistically non-significant differences compared to cells transfected with the wild type alone ($P = 0.99$, Fig. 2). The time constants were similar among these three mutants but that of I313G was larger at the membrane potential<−25 mV and smaller at >−25 mV (Fig. 3A).

The current density was also affected by the side-chain volume of amino acid residue at position 313 and a significantly larger current density was found only when I313G was co-expressed with the wild type compared with when it was expressed alone (Fig. 3B). Both the homo-tetrameric and hetero-tetrameric I313G

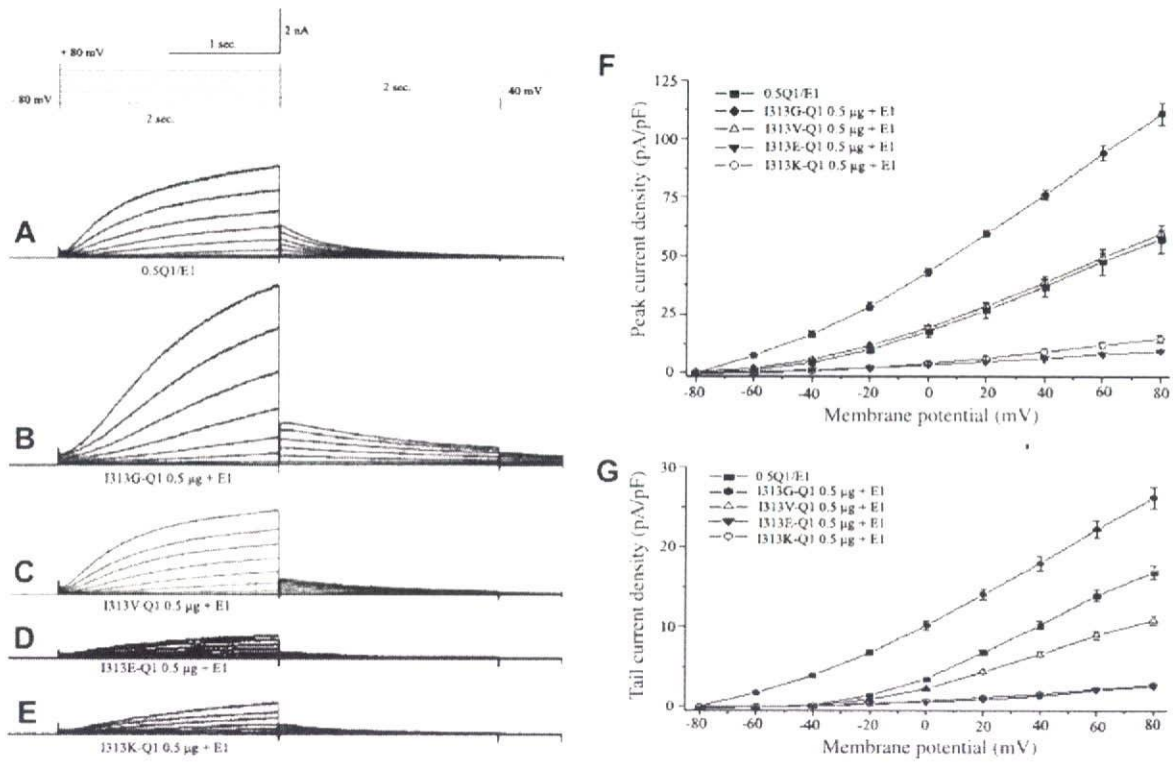


**Fig. 2.** Results of the whole-cell patch-clamp experiments in COS-7 cells. COS-7 cells were co-transfected with wild type KCNQ1 and four mutants together with KCNE1 (A–E). Current–voltage relationships are shown on the right (F,G). Augmented peak ($P < 0.001$) and tail current ($P < 0.05$) and a shift to the left in activation curve was observed when I313G was co-transfected with the wild type KCNQ1 (B and F). Dominant negative suppression was seen in D and E in which the amino acid residue was replaced by an either positive or negative charged one (D,E). Pulse protocol and graph scale are shown at the top.

with the wild type showed a shift to the left in the activation curve (Fig. 3C) suggesting a altered gating.

## Discussion

Both negatively charged (I313K) and positively charged (I313E) residues at the pore center of KCNQ1 resulted in an apparent loss of channel function when they were transfected alone (with KCNE1). The loss of function was not due to a trafficking defect and when they were co-transfected with wild type KCNQ1 (with KCNE1), a dominant negative suppression was observed.

The $I_{Ks}$ channel has six trans-membrane domains (S1–S6), a voltage sensor (S4) and a pore helix selectivity filter segment (P-loop) that connects S5 and S6 [10,17]. The selectivity filter is reflected in a highly conserved amino acid sequence for specific ion conductance as elegantly defined by the crystal structure of the bacterial KcsA channel [18] and the carbonyl oxygen atoms of these residues which bind dehydrated $K^+$ ions and act for selectivity [19,20]. An altered charge at the pore center, I313K and I313E, is expected to result in a crucial change of the electrostatic environment of the selectivity filter, with serious consequences that reduce the conduction of $K^+$ ions [21–24]. The presence of charged amino acid residues at the pore center may also disturb the closed/open equilibrium and lead to the destabilization of the open-state of the channel [25] but this was not confirmed in the present study.

The current density was also affected by the side-chain volume of the amino acid residue at the pore center (Fig. 3B and Table 1). When we substituted the neutral Isoleucine residue of KCNQ1 with Valine (I313V) which has a similar size and polarity to Isoleucine, the normalized current–voltage relationship was very similar to the wild type. The homo-tetramer of the Glycine residue (I313G) showed a reduction of the peak $K^+$ current by about 20% compared with the wild type, but the initial current was larger (Fig. 1B). Furthermore when I313G was co-expressed with the wild type KCNQ1, the $K^+$ current increased 2-fold which suggests a gain of function (Fig. 2B).

The conductive conformation of the $K^+$ channel represents a match between the ion-binding sites and the size of $K^+$ ions [26] and the filter atoms and the surrounding protein atoms are important for selective ion-binding and conduction [9,10]. The volume of side-chain residues located in position 313 may affect conduction of $K^+$ ions [27].

For the augmented $K^+$ currents observed in the I313G mutant, we postulate as follows. The homo-tetramer by the smallest amino acid residue Glycine minimized the selectivity filter size (pore) and resulted in a reduced peak current. However, when the mutant was co-transfected with the wild type, the pore was composed of mixed amino acid residue, Glycine and Isoleucine rendered the channel pore larger and augmented the $K^+$ current (Fig. 3C). Using Brownian dynamics on a simplified model of the KcsA structure, it was shown that altering the pore size of the cytosolic entrance to the selectivity filter led to a change in conductance [28].

As limitations, except for I313K, other mutants are virtual and we have no clinical counterparts so far, but if I313G is associated with short QT syndrome or not is of interest [29]. The change in ion selectivity in each mutant and the relation to the gating mechanism was not fully studied in the present report [30].

As clinical implications, the functional consequences of mutations at the pore center of KCNQ1 varied: from dominant negative suppression to a gain of function when co-transfected with wild type KCNQ1. Severe reduction of $I_{Ks}$ would be detectable as LQTS but a subtle change in $K^+$ channel function of varying degrees might go undetected.

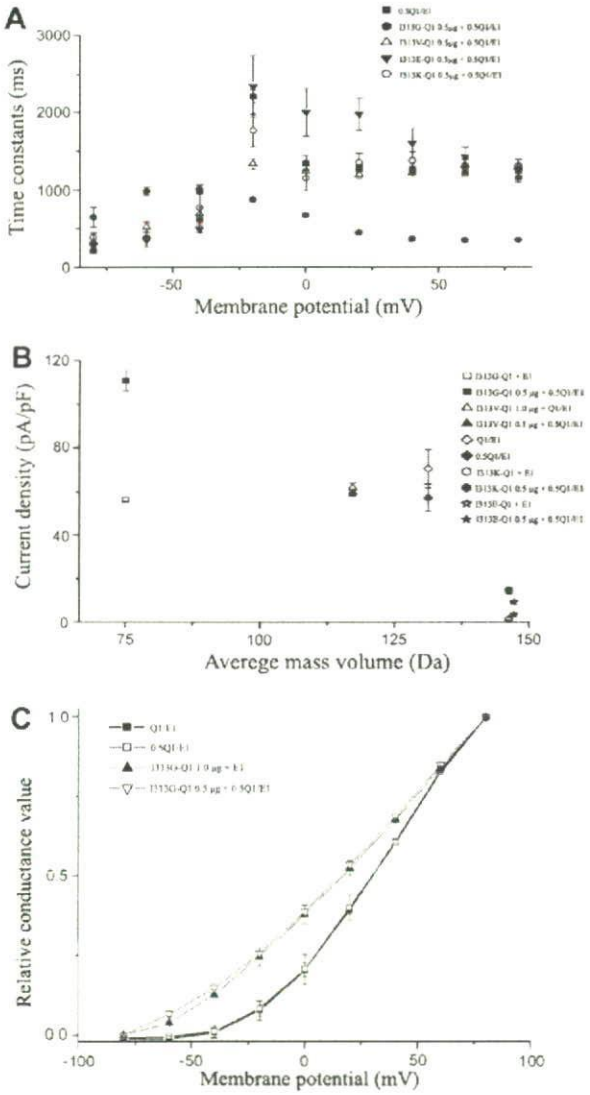


**Fig. 3.** Activation and deactivation kinetics of currents in the wild type and mutant $K^+$ channels. In A, activation and deactivation kinetics of co-expression mutants and the wild type KCNQ1 together with KCNE1 are shown. The time constants were derived from the raw current traces and plotted as the function of membrane potential. Substitution of amino acid residue at the pore center (313) altered the relation between the time constant and membrane potential. In B, currents measured at +80 mV and were plotted against the side-chain mass average volume of the residues at position 313 ($n$ = 9–19). The current was least in I313K and I313E but larger when I313G was co-expressed with the wild type. I313V was close to the wild type. In C, relative conductance of the initial tail current amplitude was similar when I313G was transfected alone or with the wild type (+KCNE1). Both shifted toward the left compared to the wild type.

In conclusion, charged residues at the pore center of KCNQ1 resulted in a loss of $K^+$ channel function and a dominant negative pattern when co-transfected with the wild type channel. The neutral residues showed zero or a small reduction of the $K^+$ current and some mutants might show a gain of function when co-expressed with the wilt type channel. Not only the site of the mutation but the alteration in charge or size seems to affect phenotype of LQTS.

## Acknowledgment

This work was supported by a grant from the Japanese Ministry of Education, Science and Culture, Tokyo, Japan.

## References

[1] J. Barhanin, F. Lesage, E. Guillemare, M. Fink, M. Lazdunski, G. Romey, K(V)LQT1 and lsK (minK) proteins associate to form the I(Ks) cardiac potassium current, Nature 384 (1996) 78–80.
[2] A.J. Moss, R.S. Kass, Long QT syndrome: from channels to cardiac arrhythmias, J. Clin. Invest. 115 (2005) 2018–2024.
[3] E. Marban, Cardiac channelopathies, Nature 415 (2002) 213–218.
[4] W. Shimizu, M. Horie, S. Ohno, K. Takenaka, M. Yamaguchi, M. Shimizu, T. Washizuka, Y. Aizawa, K. Nakamura, T. Ohe, T. Aiba, Y. Miyamoto, Y. Yoshimasa, J.A. Towbin, S.G. Priori, S. Kamakura, Mutation site-specific differences in arrhythmic risk and sensitivity to sympathetic stimulation in the LQT1 form of congenital long QT syndrome: multicenter study in Japan, J. Am. Coll. Cardiol. 44 (2004) 117–125.
[5] W. Zareba, J.A. Moss, G. Sheu, E.S. Kaufman, S. Priori, G.M. Vincent, J.A. Towbin, J. Benhorin, P.J. Svhwartz, C. Napolitano, W.J. Hall, M.T. Keating, M. Qi, J.L. Robinsdon, M.L. Andrews, International LQTS registry. Location of mutation in the KCNQ1 and phenotypic presentation of long QT syndrome, J. Cardiovasc. Electrophysiol. 14 (2003) 1149–1153.
[6] T. Ikrar, H. Hanawa, H. Watanabe, S. Okada, Y. Aizawa, M.M. Ramadan, S. Komura, F.Y. amashita, M. Chinushi, Y. Aizawa, A double point mutation in the selectivity filter site of the KCNQ1 potassium channel results in a severe phenotype, LQT1, of long QT syndrome, J. Cardiovasc. Electrophysiol. 19 (2008) 541–549.
[7] D.J. Snyders, Structure and function of cardiac potassium channels, Cardiovasc. Res. 42 (1999) 377–390.
[8] D.M. Roden, Defective ion channel function in the long QT syndrome: multiple unexpected mechanisms, J. Mol. Cell. Cardiol. 33 (2001) 185–187.
[9] S. Berneche, B. Roux, A gate in the selectivity filter of potassium channels, Structure 13 (2005) 591–600.
[10] D.A. Doyle, J.M. Cabral, R.A. Pfuetzner, A. Kuo, J.M. Gulbis, S.L. Cohen, B.T. Chait, R. MacKinnon, The structure of the potassium channel: molecular basis of $K^+$ conduction and selectivity, Science 280 (1998) 69–77.
[11] Y. Aizawa, K. Ueda, F. Scornik, J.M. Cordeiro, Y. Wu, M. Desai, A. Guerchicoff, Y. Nagata, Y. Iesaka, A. Kimura, M. Hiraoka, C. Antzelevitch, A novel mutation in KCNQ1 associated with a potent dominant negative effect as the basis for the LQT1 form of the long QT syndrome, J. Cardiovasc. Electrophysiol. 18 (2007) 972–977.
[12] Y. Hosaka, H. Nanawa, T. Washizuka, M. Chinushi, F. Yamashita, T. Yoshia, S. Komura, H. Watanabe, Y. Aizawa, Function, subcellular localization and assembly of a novel mutation of KCNJ2 in Andersen's syndrome, J. Mol. Cell. Cardiol. 35 (4) (2003) 409–415. Apr.
[13] A. Molleman, Patch Clamping: An Introductory Guide to Patch Clamp Electrophysiology, John Wiley & Sons, England, 2003. pp. 107–108..
[15] M.C. Sanguinetti, M.E. Curran, A. Zou, J. Shen, P.S. Spector, D.L. Atkinson, M.T. Keating, Coassembly of K(V)LQT1 and minK (IsK) proteins to form cardiac I(Ks) potassium channel, Nature 384 (1996) 80–83.
[16] I.R. Boulet, A.L. Raes, N. Ottschytsch, D.J. Snyders, Functional effects of a KCNQ1 mutation associated with the long QT syndrome, Cardiovasc. Res. 70 (2006) 466–474.
[17] G. Seebohm, N. Strutz-Seebohm, O.N. Ureche, R . Baltaev, A. Lampert, G. Kornichuk, K. Kamiya, T.V. Wuttke, H. Lerche, M.C. Sanguinetti, F. Lang, Differential roles of S6 domain hinges in the gating of KCNQ potassium channels, Biophys. J. 90 (2006) 2235–2244.
[18] A.D. Wei, A. Butler, L. Salkoff, KCNQ-like potassium channels in *Caenorhabditis elegans* conserved properties and modulation, J. Biol. Chem. 280 (2005) 21337–21345.
[19] J.A. Smith, C.G. Vanoye, A.L. George Jr., J. Meiler, C.R. Sanders, Structural models for the KCNQ1 voltage-gated potassium channel, Biochemistry 46 (2007) 14141–14152.
[20] T.W. Allen, A. Bliznyuk, A.P. Rendell, S.H. Kuyucak, The potassium channel: structure, selectivity and diffusion, J. Chem. Phys. 112 (2000) 8191–8204.
[21] J. Aqvist, V. Luzhkov, Ion permeation mechanism of the potassium channel, Nature 404 (2000) 881–884.
[22] S.Y. Noskov, S. Bernèche, B. Roux, Control of ion selectivity in potassium channels by electrostatic and dynamic properties of carbonyl ligands, Nature 431 (2004) 830–834.
[23] Y. Zhou, R. MacKinnon, The occupancy of ions in the $K^+$ selectivity filter: charge balance and coupling of ion binding to a protein conformational change underlie high conduction rates, J. Mol. Biol. 333 (2003) 965–975.
[24] D. Bichet, M. Grabe, Y.N. Jan, L.Y. Jan, Electrostatic interactions in the channel cavity as an important determinant of potassium channel selectivity, Proc. Natl. Acad. Sci. USA 103 (2006) 14355–14360.
[25] G. Seebohm, P. Westenskow, F. Lang, M.C. Sanguinetti, Mutation of colocalized residues of the pore helix and transmembrane segments S5 and S6 disrupt deactivation and modify inactivation of KCNQ1 $K^+$ channels, J. Physiol. 563 (2005) 359–368.
[26] S.W. Lockless, M. Zhou, R. MacKinnon, Structural and thermodynamic properties of selective ion binding in a K+ channel, PLoS Biol. 121 (2007) 1079–1088.
[27] L.J. Mullins, An analysis of pore size in excitable membranes, J. Gen. Physiol. 43 (1960) 105–117.
[28] S.H. Chung, T.W. Allen, S. Kuyucak, Conducting-state properties of the KcsA potassium channel from molecular and Brownian dynamics simulations, Biophys. J. 82 (2002) 628–645.

[29] C. Bellocq, A.C. Ginneken, C.R. Bezzina, M. Alders, D. Escande, M.M. Mannens, I. Baró, A.A. Wilde, Mutation in the KCNQ1 gene leading to the short QT-interval syndrome, Circulation 109 (2004) 2394–2397.

[30] T. Lu, A.Y. Ting, J. Mainland, L.Y. Jan, P.G. Schultz, J. Yang, Probing ion permeation and gating in a $K^+$ channel with backbone mutations in the selectivity filter, Nat. Neurosci. 4 (2001) 239–246.